High performance fiber-Fabry-Perot resonator targeting quantum optics applications

Jonathan P. Hedger, Tino Elsmann, Martin Becker, Tobias Tiess, Andre N. Luiten, and Ben M. Sparkes

Quantum optics experiments frequently require the separation of single-photon-level signals from strong classical fields. In circumstances in which the signals are spectrally close, and one cannot make use of relatively simple separation methods based around differences in polarization state, optical mode, or beam direction, it is necessary to exploit the frequency difference itself as the means for signal separation. We have constructed and characterized an efficient and robust fiber-based filter, consisting of an all-fiber Fabry-Perot resonator, to achieve this goal. Our filter shows 31 dB of suppression of unwanted signals and 76% transmission of the desired signal. The transmission of the filter was stabilized to within 2% of its maximum for over 35 hours through simple temperature stabilization.

***Index Terms*—Fabry-Perot resonators, Optical filters, Optical resonators, Quantum optics, Spectral filter**

I. Introduction

IT is frequently the case in quantum optics experiments that one is faced with the need to separate a single-photon-level "probe" signal from a co-propagating high-power "control" field. Examples of this occur when using the ground-states of alkali atoms to encode or manipulate quantum or classical information (Fig. 1) such as with highly-efficient quantum memories [1], or precision atom interferometry [2]. These ground-states are often used because their long coherence times can preserve quantum information for seconds [3]. These types of experiments necessitate isolation of the probe field from the control field so as to preserve its quantum information. While it is sometimes possible to use relatively simple separation approaches, such as differences in polarization, timing, or spatial modes between the fields, this is not always the case. This may occur because the specifics of the atom-light interaction demand that these characteristics are shared, or simply because of the presence of a large number of classical fields. In this case, the experimenter is forced to separate these signals based on the differences in their frequencies alone and is thus in need of a high-performance spectral filter. There are three key challenges here: (a) the transmission of the probe must be very high so that the quantum information is preserved, (b) the rejection of the control, which can be as close in frequency as a few GHz, also needs to be very high, and (c) both the rejection and transmission of the optical filter needs to be stable over time.

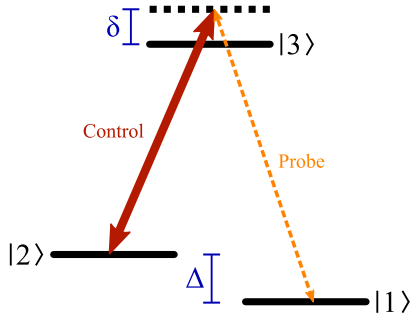

Fig. 1. A Λ-system formed between two atomic ground-states and one excited-state, where δ is the one-photon detuning from resonance, and Δ is the ground-state separation. For rubidium-85 Δ = 3 GHz, rubidium-87 Δ = 6.8 GHz, and caesium-133 Δ = 9.2 GHz.

The conventional approach is to use free-space optical resonators, which can provide strong filtering of the control while delivering high transmission of the probe. One extreme example of this is the vacuum-isolated ultra-high-finesse resonator with a sub-Hz linewidth [4]. Although this delivers excellent spectral separation, the challenge with such a narrow resonance is the very tight frequency locking that is necessary. There is therefore an inherent trade-off between the extinction (ratio of transmission to rejection) and the difficulty of the frequency stabilization. This is a significant challenge in single-photon-level experiments, which can require data to be collected over many hours and thus need to be stable over these periods. The solution must also have a large operational range to accommodate for three-level atomic experiments which have a one-photon detuning from the excited-state ranging from zero [1] to tens of GHz [5].

The traditional implementation of a spectral filter in the field of quantum optics is based on a solid etalon with reflective coatings [6]–[9]. These filters have been shown to provide suppression up to 45 dB for signals separated by a few GHz, while also showing a resonant frequency instability on the 1 to 10 MHz level over multiple hours [6], [8]. By cascading two of these resonators it is possible to provide $>$ 100 dB of control field suppression at the expense of only a few percent probe transmission [7]. The advantage of using multiple cavities is that the finesse of each need only be moderate while still delivering excellent suppression. This comes at the cost of higher complexity and more susceptibility

Manuscript received; revised.

This work was supported by Australian Research Council (DE170100752); BMBF framework for innovative growth core TOF (03WKCV03E); South Australian Government through the Premier's Research and Industry Fund. *(Corresponding author: Ben Sparkes)*

J. P. Hedger, A. N. Luiten and B. M. Sparkes are with the Institute for Photonics and Advanced Sensing (IPAS) in the School of Physical Sciences at the University of Adelaide, Adelaide, 5005, SA, Australia (e-mail: jonathan.hedger@adelaide.edu.au, andre.luiten@adelaide.edu.au, ben.sparkes@adelaide.edu.au)

T. Elsmann, M. Becker and T. Teiss are with Leibniz Institute of Photonic Technology (IPHT), Albert-Einstein-Str. 9, 07745 Jena, Germany (email: tino.elsmann@leibniz-ipht.de, martin.becker@leibniz-ipht.de, tobias.tiess@leibniz-ipht.de)

to alignment fluctuations. Such work highlights the potential of cascading cavities if there were a means to obtain high cavity transmission and low-loss concatenation.

Compared to free-space optics, optical fiber is a more robust and compact platform for many applications. Single-mode fiber provides inherent spatial mode filtering capabilities and is easily interfaced to other fiber-coupled quantum technologies [10], including work mediating ultra-strong atom-light interactions directly on fiber platforms [2], [5], [9], [11]. Past fiber-based Fabry-Perot resonators have been constructed using a variety of methods [12]–[15]. Each of these approaches has its individual set of merits, for example one approach using two separate FBGs achieved a peak transmission of approximately 75% [15], while another using the polished and coated ends of two fibers showed a finesse of 37,000 [13]. These experimental efforts, however, have not been able to produce a device capable of simultaneously providing high transmission with a finesse sufficient for filtering the control, but not so high as to hinder long term stability. However, they do point towards the advantages of using fiber as the medium for implementing the Fabry-Perot rather than free-space optics.

Here we present a spectral filter targeting quantum optics applications formed within a fiber using two custom-designed FBGs that have been chosen to provide high transmission and a large finesse in a compact, robust, and stable package. The filter showed 31 dB of suppression with a peak transmission of 76%. We measured the instability of the resonant frequency of the transmission peak over 35 hours, finding a root mean square (rms) deviation of 2.84 MHz, equivalent to fluctuations of less than 2% in transmitted power. This was achieved through simple temperature stabilization of the fiber.

II. Fiber Fabry-Perot Fabrication

The goal was to create a resonator with effective mirrors of $R = 0.98$, and a free-spectral-range (FSR) of 6 GHz (i.e. twice the hyperfine ground-state splitting of rubidium-85). The resonator appears in the spectral region in which both FBGs are reflective, given by [16]

$$R(\lambda) = \frac{\kappa^2 \sinh^2 \gamma L}{\gamma^2 \cosh^2 \gamma L + \Delta\beta^2 \sinh^2 \gamma L}, \tag{1}$$

where $L = \Lambda\left(m + \frac{1}{2} - \frac{\phi}{\pi}\right)$ is the physical length of the grating, Λ is the period of the grating, m is the integer number of periods contained in the grating with $\phi = 0$, $\kappa = \delta n\pi/\lambda$ is the coupling coefficient of the grating, δn is the depth of the grating, λ is the wavelength of the light, $\Delta\beta$ is the detuning and $\gamma^2 = \kappa^2 - \Delta\beta^2$. We desire this operational range to be approximately 200 GHz wide to accommodate a variety of one-photon detunings, requiring short and deep FBGs.

Within the operational window determined by Eq. 1 the transmission T of an optical field through the fiber Fabry-Perot (FFP) is governed by [17]

$$T(f) = \frac{(1-R_1)(1-R_2)V}{\left(1-\sqrt{R_1R_2}V\right)^2 + 4\sqrt{R_1R_2}V\sin^2\left(\frac{f-f_{os}}{FSR}\pi\right)}, \tag{2}$$

where R_1 and R_2 are the individual reflectivities of the two FBGs at frequency f, f_{os} is the centre frequency of the resonator, and $V = 1 - \alpha$, where α is the single-pass intracavity intensity loss. The $FSR = c/(2nl)$ depends on the spatial separation l between the two FBGs, and the speed of light inside the fibre c/n, where the refractive index $n = 1.45$ at 795 nm. It can be seen from Eq. 2 that, when on resonance, if $R_1 \neq R_2$ or $V < 1$, then the maximum transmission of the resonator will be reduced from unity. The finesse of the FFP resonator $\mathcal{F} = \pi/\left|\ln\sqrt{R_1R_2}V\right|$ determines how effectively it can suppress the unwanted control field [17].

To achieve the requirements listed above, the FFP resonator was designed with two 1-mm-long FBGs each with a grating depth of $\delta_n \approx 0.0007$, separated by 17.7 mm. The gratings were inscribed by a two-beam phase-mask interferometer in combination with a fs-laser system. The laser had a 1 kHz repetition rate with 170 fs long pulses. The pulse energy was optimized for the experiment to be within 240 μJ and 250 μJ at a wavelength of 267 nm. The first diffraction orders were reflected by rotatable mirrors and formed the FBG structure through an interference pattern at the fiber. The grating period, and therefore the final Bragg wavelength, was tuned with high accuracy by rotating the mirrors (for more details see Ref. [18]). In our case the interferometer was adjusted to inscribe gratings with a final reflection wavelength of $\lambda_0 = 795.0 \pm 0.1$ nm into the different fibers to match the D1 line of rubidium. By inserting a slit aperture into the beam path, the grating length was set to be 1 ± 0.1 mm.

Grating strength was monitored during inscription by measuring transmitted light through the FBGs with a broadband light source at 800 nm and an optical spectrum analyzer. The inscription time was adapted for each individual FBG to best match grating pairs in terms of $R(\lambda_0)$. The individual transmission spectra of the two gratings could be observed during the inscription process due to the thermal load experienced by the FBG under illumination. This load resulted in an approximately 1 nm shift of the second FBG centre wavelength while illuminated. The distance between the gratings was controlled by a linear motor stage which pulled the fiber 17.700 ± 0.002 mm after writing the first grating.

The FFPs were written in the direction of the fast axis of polarization-maintaining (PM) fiber to better preserve the polarization properties of the probe signal. Due to the non-symmetric refractive index profile of PM-fiber, a single physical FBG will have a different central wavelength and reflectivity in each polarization axis. To improve the real-time monitoring, a PM-isolator with a suppression of better than 25 dB was spliced between the unpolarized light source and the PM-fiber to block the fast axis light. This ensured that only the FBGs in the slow axis were observed.

III. Results

We characterized the performance of a number of FFPs inscribed using the above method in two domains: firstly measuring their transmission, and secondly their long-term stability. Transmission was tested using the set-up shown in Fig. 2. The individual characteristics of the FBGs were determined by measuring the full scattering matrix of the FFP as a function of frequency.

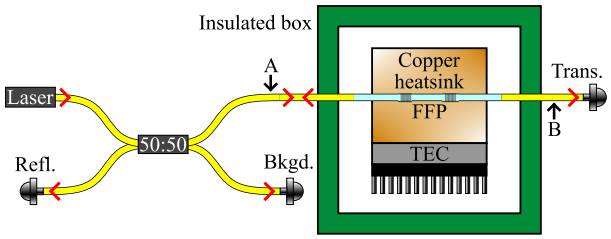

Fig. 2. Experimental characterization set-up. 50:50 - 50:50 non-polarizing fiber beam splitter; Refl. - reflection detector, Trans. - transmission detector, Bkgd. - background detector, TEC - Thermo-electric cooler, red arrows - light propagation direction. Points A and B refer to where additional polarization filtering was implemented for the suppression measurements, with a Wollaston prism inserted at A, and a Glan-Thompson polarizer inserted at B.

The characterization itself is based on measuring the reflected and transmitted optical power of the FFP from both ends of the resonator while the laser is scanned across two FFP resonances. To obtain an accurate normalization of the transmission and reflection coefficients we measured the incident power by splitting the input light with a 50:50 fiber splitter. The light reflected off the FFP was measured after travelling back through the 50:50 fiber splitter. The reflected and transmitted signals were then fitted according to the spectral response of a two mirror resonator from Eq. 2. We found that, for the FFP with the highest transmission efficiency (Fig. 3(a)), $R_1 = 0.9808 \pm 0.0004$, $R_2 = 0.9637 \pm 0.0010$, and $\alpha = 0.0033 \pm 0.0001$. The uncertainties were derived from the standard deviation of 5 measurements.

Equation 2 predicts that with the values extracted for our FFP we should achieve up to 36 dB of relative suppression between the control and probe. However, with no polarization filtering applied we measured a maximum suppression of 23 dB in the slow axis resonator. This is due to cross-talk between the two possible resonators that are formed in each of the optical axes of the PM-fiber. The inset of Fig. 3(a) shows a combination of the resonators of both polarization axes, where the slow axis has a high finesse ($\mathcal{F} = 106$), while the fast axis has a low finesse ($\mathcal{F} \approx 3$). The extinction ratio between the fast and slow axes in the PM-fiber used is specified as 20 dB, which means that some small fraction of the light in the slow axis of the PM-fiber will enter the low finesse resonator and reduce the observed suppression of the control. There will also be some cross-talk between the axes due to the imperfections in the FBGs, exaggerated by the strength of these gratings. Adding polarization filtering both before and after the FFP, as indicated in Fig. 2, removes the fast axis cross-talk and improved this result to 31 dB (Fig. 3(b)).

The second part of characterising the FFP relates to its long-term frequency instability, caused by changes to strain

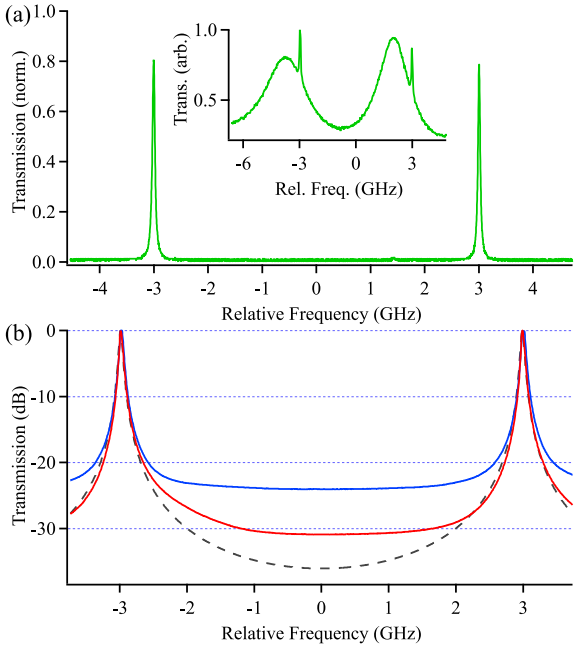

Fig. 3. (a) Transmission of the high finesse mode through the FFP. Inset shows transmission of the resonator in both polarization axes at once. (b) Transmission in dB, with no post-filtering (blue), with post-filtering using a Glan-Thompson polariser (red), and the theoretical response (dashed grey).

and temperature. Without any temperature stabilisation, the FFP showed drifts of 3.7 GHz/K. The measured rms room temperature fluctuations (see inset in Fig 4) were ≈ 0.2°C which would have led to GHz-scale fluctuations in the resonant frequency of the filter. A copper block 1x1x6 cm in size was used to encase the resonator region of the fiber and was temperature stabilised using a PID controller with a stated stability of 2 mK. The fiber and copper block were placed inside an aluminum box with fibre joiners inserted into the walls to reduce the effect of strain on the system. This, in turn, was placed inside an insulated box to further isolate the FFP from fluctuations in room temperature.

To measure the frequency drift of the FFP we recorded the transmitted light field as a function of frequency relative to a rubidium reference cell. This was logged every 10 minutes over 35 hours. The FFP showed 2.84 MHz rms deviation over this time period, with a total drift of 10 MHz. This is equivalent to less than 2% fluctuations of transmitted power at 76% peak transmission with a 60 MHz FWHM.

IV. Discussion

While 76% transmission is higher than similar free-space filter systems [6]–[9], improved transmission is still desired. The maximum transmission of the fiber characterised above was limited mainly by the intra-cavity loss α. Comparing multiple FFPs created using the method described above, we found that α can be as low as 0.00067. There are three main factors that contribute to this loss. The first is imperfections in FBG inscription, leading to coupling of light into the cladding [19]. These losses could be reduced by lowering the depth of the FBGs and extending their length to compensate, at the expense of FFP bandwidth. For example, if the grating depth

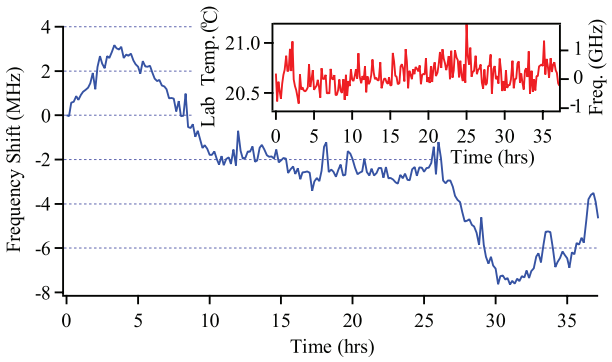

Fig. 4. Frequency of laser locked to FFP measured relative to a rubidium reference cell. Inset shows laboratory temperature and equivalent FFP frequency drift.

was halved and the length doubled to 2 mm to maintain reflectivity, the FFP bandwidth would be halved. The second main loss factor is ultra-violet (UV)-induced photo-darkening [20]. This effect could be greatly reduced by applying homogeneous UV illumination following inscription.

With matching reflectivities of $R = 0.98$, a 2 mm FBG length, and a conservative $\alpha = 0.001$, we would expect a transmission of 90% with a relative suppression of 40 dB. With transmission at this level, multiple FFPs could be concatenated together to increase the suppression without significant loss of signal. A typical quantum optics experiment requires roughly 90 dB of suppression of the control field to separate single-photon-level signals faithfully [7], [9]. Splicing together three FFP resonators with $R = 0.98$, separated by circulators, would provide 120 dB of suppression with 50% probe transmission. The circulators allow each FFP to be interrogated individually to set their resonant temperature while providing isolation to remove undesired etalons forming between the FFPs. The overall transmission will mostly be limited by the approximately 1 dB insertion loss of commercially-available circulators, with each splice adding approximately 0.01 dB.

Here, suppression of the control is limited by polarization cross-talk between the high and low finesse polarization axes. This could be overcome by writing the gratings into PM-fiber that has a better polarization extinction ratio (up to 30 dB possible), or ensuring that both axes have relatively high finesse resonators. Of the other FFPs characterized, some showed $\mathcal{F} > 30$ in both axes, which would improve relative suppression to over 38 dB.

V. Conclusion

We have created an efficient and robust fiber-based optical filter based on a fiber Fabry-Perot resonator. Our FFP showed 31 dB of suppression and 76% transmission, with less than 2% power fluctuations over 35 hours using only simple temperature stabilization. Small changes to the design process, such as reducing the depth and increasing the length of the FBGs, and applying homogeneous UV illumination following inscription, would significantly improve the performance. This opens the way for compact optical systems involving multiple fiber resonators, which can deliver low loss with exceedingly high spectral extinction.

Acknowledgment

The authors thank Lily Taylor and Madison Simmonds for their contribution to the fiber Fabry-Perot characterization and testing. This work was performed, in part, at the Optofab node of the Australian National Fabrication Facility, a company established under the National Collaborative Research Infrastructure Strategy to provide nano and micro-fabrication facilities for Australia's researchers.

References

[1] Y.-F. Hsiao, P.-J. Tsai, H.-S. Chen, S.-X. Lin, C.-C. Hung, C.-H. Lee, Y.-H. Chen, Y.-F. Chen, I. A. Yu, and Y.-C. Chen, "Highly efficient coherent optical memory based on electromagnetically induced transparency," *Physical Review Letters*, vol. 120, p. 183602, 2018.

[2] M. Xin, W. S. Leong, Z. Chen, and S.-Y. Lan, "An atom interferometer inside a hollow-core photonic crystal fiber," *Science Advances*, vol. 4, 2018.

[3] S.-J. Yang, X.-J. Wang, X.-H. Bao, and J.-W. Pan, "An efficient quantum light-matter interface with sub-second lifetime," *Nature Photonics*, vol. 10, p. 381, 2015.

[4] B. C. Young, F. C. Cruz, W. M. Itano, and J. C. Bergquist, "Visible lasers with subhertz linewidths," *Phys. Rev. Lett.*, vol. 82, pp. 3799–3802, 1999.

[5] M. R. Sprague, P. S. Michelberger, T. F. M. Champion, D. G. England, J. Nunn, X.-M. Jin, W. S. Kolthammer, A. Abdolvand, P. S. J. Russell, and I. A. Walmsley, "Broadband single-photon-level memory in a hollow-core photonic crystal fibre," *Nature Photonics*, vol. 8, p. 287, 2014.

[6] P. Palittapongarnpim, A. Macrae, and A. I. Lvovsky, "Note: A monolithic filter cavity for experiments in quantum optics.," *Review of Scientific Instruments*, vol. 83, p. 066101, 2012.

[7] C. Kupchak, T. Mittiga, B. Jordaan, M. Namazi, C. Nölleke, and E. Figueroa, "Room-temperature quantum memory for polarization states," *Scientific Reports*, vol. 5, p. 7658, 2014.

[8] A. Ahlrichs, C. Berkemeier, B. Sprenger, and O. Benson, "A monolithic polarization-independent frequency-filter system for filtering of photon pairs," *Applied Physics Letters*, vol. 103, no. 24, p. 241110, 2013.

[9] T. Peters, T.-P. Wang, A. Neumann, L. S. Simeonov, and T. Halfmann, "Single-photon-level narrowband memory in a hollow-core photonic bandgap fiber," *Opt. Express*, vol. 28, pp. 5340–5354, 2020.

[10] C. M. Natarajan, M. G. Tanner, and R. H. Hadfield, "Superconducting nanowire single-photon detectors: physics and applications," *Superconductor Science and Technology*, vol. 25, p. 063001, 2012.

[11] F. Blatt, T. Halfmann, and T. Peters, "One-dimensional ultracold medium of extreme optical depth," *Optics Letters*, vol. 39, p. 446, 2014.

[12] Y. Qi, C. Jia, L. Tang, M. Wang, Z. Liu, and Y. Liu, "Simultaneous measurement of temperature and humidity based on FBG-FP cavity," *Optics Communications*, vol. 452, pp. 25–30, 2019.

[13] Y. Colombe, T. Steinmetz, G. Dubois, F. Linke, D. Hunger, and J. Reichel, "Strong atom-field coupling for Bose-Einstein condensates in an optical cavity on a chip," *Nature*, vol. 450, no. 7167, pp. 272–276, 2007.

[14] J. Canning and M. G. Sceats, "π-phase-shifted periodic distributed structures in optical fibres by UV post-processing," *Electronics Letters*, vol. 30, pp. 1344–1345, 1994.

[15] J. H. Chow, I. C. M. Littler, G. de Vine, D. E. McClelland, and M. B. Gray, "Phase-sensitive interrogation of fiber Bragg grating resonators for sensing applications," *Journal of Lightwave Technology*, vol. 23, no. 5, pp. 1881–1889, 2005.

[16] A. Melloni, M. Floridi, F. Morichetti, and M. Martinelli, "Equivalent circuit of Bragg gratings and its application to Fabry-Pérot cavities," *Journal of the Optical Society of America A*, vol. 20, p. 273, 2003.

[17] N. Hodgson and H. Weber, "The Fabry Perot resonator," in *Optical Resonators*, ch. 4, pp. 189–215, Springer-Verlag London, 1997.

[18] M. Becker, T. Elsmann, A. Schwuchow, M. Rothhardt, S. Dochow, and H. Bartelt, "Fiber Bragg gratings in the visible spectral range with ultraviolet femtosecond laser inscription," *IEEE Photonics Technology Letters*, vol. 26, p. 1653, 2014.

[19] T. Erdogan, "Fiber grating spectra," *Journal of Lightwave Technology*, vol. 15, pp. 1277–1294, 1997.

[20] J. Fiebrandt, S. Jetschke, M. Leich, and H. Bartelt, "UV-induced photodarkening and photobleaching in UV-femtosecond-pulse-written fibre bragg gratings," *Laser Physics Letters*, vol. 10, p. 085102, 2013.